International Journal of Heat and Technology
Vol. 44, No. 2, April, 2026, pp. 793-802
Journal homepage: http://iieta.org/journals/ijht

# Density Functional Theory Based Study of Hydrogen Cyanide Interaction with Graphene Modified by Ni, Si, S and Co for Sensor Applications

Salah Abdul Mahdi Khudair

Directorate General of Education in Babylon Governorate, Ministry of Education, Babylon 51001, Iraq

Corresponding Author Email: salahalmahdi30@gmail.com



https://doi.org/10.18280/ijht.440229

**Received:** 2 February 2026
**Revised:** 14 April 2026
**Accepted:** 21 April 2026
**Available online:** 30 April 2026

***Keywords:***
*electronic properties, gas adsorption, graphene-based sensors, toxic gas detection*

**ABSTRACT**

Hydrogen cyanide (HCN) is one of the most toxic gases: it is necessary to identify it and continuously monitor it as an indicator of industrial safety, environmental control, and human safety. The given study, based on first-principles density functional theory (DFT) computations to study the adsorption of HCN on graphene (Gr) doped with nickel (Ni), sulfur (S), silicon (Si), and cobalt (Co) atoms, is systematic. Structural optimization, adsorption energy ($E_{ad}$), charge-transfer analysis, density of states (DOS), and frontier molecular orbital (FMO) mapping have been used to explain the mechanism of interaction. The results indicate that there is a significant change in the adsorption characteristics of Gr due to doping, whereby stronger adsorption was observed (i.e., negative adsorption energies), changes in the DOS were observed, and significant charge transfer was observed in both Ni-doped Gr (Ni-Gr) and Si-doped Gr (Si-Gr). Also, the HOMO/LUMO orbitals showed strong localization around the dopant site and the HCN molecule, which is indicative of enhanced chemisorption. Co-doped Gr (Co-Gr) and S-doped Gr (S-Gr), on the other hand, showed reduced physisorption and reduced electronic structural perturbation. These findings indicate that a controlled doping of Gr is an effective method to increase its selectivity and sensitivity to HCN, which can be used to draw valuable conclusions in the development of more sophisticated Gr-based sensors.

## 1. INTRODUCTION

The necessity to have highly selective and sensitive gas sensors capable of detecting lethal gases at trace concentrations has been heightened by the growing concern over chemical safety and air quality all over the globe [1-3]. Hydrogen cyanide (HCN) is a volatile and highly toxic chemical that is very dangerous to human health and environmental systems because it is used extensively in industrial processes, mining, and could be used in chemical warfare [4, 5]. Widely used cyanide substances, e.g., HCN, may pass into the body via different pathways [6] and influence oxygen uptake [7]. Though HCN is widely applied in industries and the agricultural sector [8], it is considered a threat to safety. Specifically, 5.6%-12.8% atmospheric concentrations can result in spontaneous aggregation, which can lead to explosive reactions [9, 10].

Therefore, effective sensing systems to monitor HCNs are of utmost significance both in the civilian and defense environment [11]. Gr is a 2D-carbon (C)-based nanomaterial, to which a lot of attention has been paid because of the high surface area, high electrical conductivity, and chemical tunability, rendering it an important material in gas sensing applications [12]. But pristine Gr has quite low physisorption of most gas molecules, including HCN, therefore limiting its intrinsic sensitivities. To overcome this, researchers have been using more heteroatomic doping and molecular functionalization. These methods are very useful in modifying the electronic properties and surface chemistry of Gr, and increase its chemical reactivity and adsorption properties [13-18].

Single-atom catalysts, substitutional dopants, and molecular linkers not only create localized active sites that strongly interact with target analytes but also modulate the density of states (DOS) near the Fermi level, thereby enabling transduction mechanisms based on charge-transfer-induced changes in conductance [19, 20]. Comparing pristine Gr, Co-anchored Gr sheets show much higher adsorption energies toward $SO_2$, NO, CO, $NH_3$, and HCN. This leads to noticeable changes in electrical conductivity, which could be used for sensing [21, 22]. The addition of defects as well as dopants changes the material from semiconducting to semi-metallic state and raises the adsorption energy ($E_{ad}$) of HCN, significantly enhancing sensitivity, according to the latest density functional theory (DFT) studies of B- and P-co-doped armchair Gr nanoribbons [23, 24]. Notwithstanding such developments, there is currently no comparative, systematic theoretical study of HCN adsorption on the Gr modified through atomic silicon (Si), nickel (Ni), cobalt (Co), and sulfur (S) dopants.

In order to bridge the gap between sensor performance and material design, DFT calculations can be used to give an atomistic model of quantifying adsorption geometries, charge transfer, energetics, and modifications in electronic structure

[25, 26]. In this case, we apply DFT to analyze the interaction of HCN gas with Gr sheets doped with different elements and functional groups such as Si, S, Ni, and Co. The reason behind the choice of these dopants is that they possess some special electronic properties and have been demonstrated to alter the adsorption properties of C nanomaterials [27, 28].

A potent knob for tuning the surface chemistry and electronic structure of graphene is hetero-atom doping [29, 30]. With an emphasis on their consequences with regard to gas sensing performance, our goal is to present a mechanistic and comparative knowledge regarding how each dopant affects the system's electronic behavior, $E_{ad}$, and charge transfer. The knowledge gained from the presented research is intended to aid in the rational design of Gr-based sensing materials tuned for selective and sensitive detection of toxic gases such as HCN [31-33]. The presented study closes that gap by offering quantitative recommendations for sensor engineering.

## 2. COMPUTATIONAL METHODS

GaussView 5.0 is used for the purpose of showing the results related to all first-principles calculations, which are conducted using DFT [36] as implemented in the specific software package Gaussian [34-36]. With this approach, our optimized structures can be observed. The generalized gradient approximation (GGA) in the form of the Perdew-Burke-Ernzerhof (PBE) functional has been utilized to analyze electron exchange and correlation interactions. The basis set regarding this GGA was 6-31G.

Moreover, bond angles, bond lengths, and binding energies, among other parameters, could be calculated with the use of this functional method [9, 37]. The results of the DOS are obtained with the use of GaussSum software [38]. In Gr supercells with 42 C atoms, doped Gr models are made by replacing one central C atom with a dopant atom (Ni, Si, S, or Co). This configuration is associated with a dopant concentration of about 2.4%, which is the lowest possible level of dopant-dopant interaction without distorting the intrinsic structure of Gr sheet [39]. $E_{ad}$ of the HCN molecule on doped Gr surfaces was calculated ($E_{ad\,(gas\,+\,doped\,-\,Gr)}$) using the equation [27, 40, 41]:

$$E_{\mathrm{ad}\,(gas+\mathrm{doped-Gr})} = E_{(gas+\mathrm{doped-Gr})} - [E_{\mathrm{doped-Gr}} + E_{gas}] \quad (1)$$

In this equation, $E_{(gas\,+\,doped\,-\,Gr)}$ represents the total energy regarding the relaxed molecule on doped-Gr, $E_{doped\text{-}Gr}$ represents the energy of isolated doped-Gr surfaces, whereas $E_{gas}$ represents the energy of the gas molecule in its isolated form. The interaction mechanism is interpreted based on the variation in frontier molecular orbital (FMO) energies, namely, the highest occupied molecular orbital (HOMO) and the lowest unoccupied molecular orbital (LUMO) between the isolated surfaces and the gas-adsorbed configurations. Due to its electron-rich nature, the HOMO functions as an electron donor, whereas the LUMO, being electron-deficient, serves as an electron acceptor [42].

## 3. RESULTS AND DISCUSSION

Gr supercells composed of a 3 × 3 unit cell were constructed to minimize periodic image interactions [43]. Single-atom doping was performed through substituting a central C atom with a dopant atom [44] (Ni, Si, S, or Co), resulting in a structurally stable configuration on the Gr surface prior to the investigation of HCN adsorption.

This atomic substitution, as shown in Figure 1, causes small geometric distortions in the local structure of the Gr lattice, meaning that the incorporation of dopants has a moderate effect on the surface morphology [45].

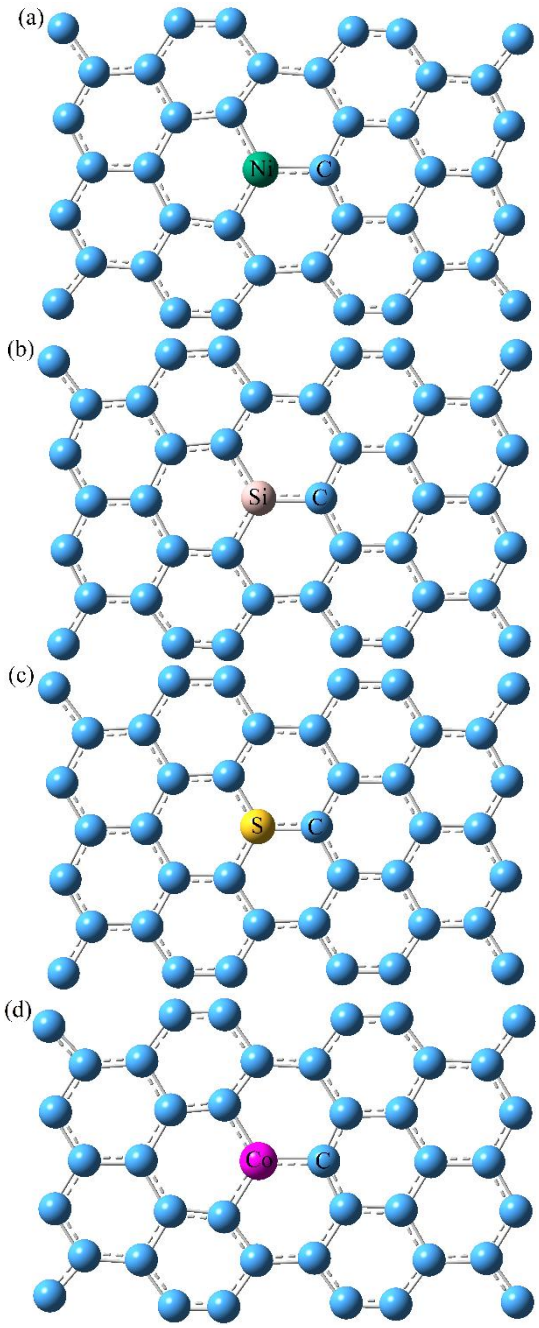


**Figure 1.** Optimized lattice structures of doped Gr systems with (a) Ni, (b) Si, (c) S, and (d) Co atoms

The optimized bond lengths between the dopant atoms and those of their neighboring C atoms have been determined to be 1.69 Å for Ni–C [46], 1.60 Å for Si–C [47], 1.50 Å for S–C, and 1.64 Å for Co–C. These values are quite consistent with those reported in the earlier literature, which proves the validity of the structures of the substitutional doping. Amazingly, the doped Gr systems that had an initial input of

these foreign atoms maintained a general planar morphology following the complete structural relaxation, demonstrating that the modifications do not severely disrupt the integrity of the Gr lattice [48]. Table 1 shows the electronic properties of Gr doped by different atoms (Ni, Si, S, and Co).

**Table 1.** Presents a comparative summary of the electronic properties of the doped Gr-based sensor models

| Materials | $E_g$ (eV) | $E_{HOMO}$ (eV) | $E_{LUMO}$ (eV) | $E_F$ (eV) |
|---|---|---|---|---|
| Ni–Gr | 0.034 | -5.566 | -5.532 | -5.549 |
| Si–Gr | 0.030 | -5.339 | -5.309 | -5.324 |
| S–Gr | 0.311 | -5.284 | -4.973 | -5.128 |
| Co–Gr | 0.129 | -4.969 | -4.840 | -4.904 |

Note: Energy gap ($E_g$); Highest occupied molecular orbital (HOMO); Lowest unoccupied molecular orbital (LUMO); Fermi energy ($E_F$).

The Fermi energy ($E_F$), LUMO and HOMO energy levels and the corresponding energy gap ($E_g$) of each doped configuration have been reported in Table 1. These parameters demonstrate that the different dopants selectively modulate the electronic structure of Gr, which could indicate the tunable behavior, which is essential for its performance in the sensors. The measured range of $E_g$ of 0.030-0.311 eV in the doped Gr systems shows a lot of potential in gas sensing applications, particularly in trace levels of toxic gases such as HCN [49]. Materials that have such small band gaps, in particular, are highly susceptible to surface adsorption processes [50], with any small perturbations in the local electronic environment leading to detectable changes in conductivity or Fermi level position [51].

A narrow and finite gap facilitates easier electron excitation between the conduction and valence bands, thus enhancing the electrical response of the material to adsorbed molecules. This high sensitivity is important in applications where the low-concentration analytes are to be detected [52]. Furthermore, the moderate gap values in this case are a desirable balance sufficiently wide for suppressing background electrical noise, but narrow enough to provide high conductivity and reactivity [53].

Within the sensor design context, this band gap range enables fast charge transfer dynamics and significant changes in electronic properties in response to gas adsorption, which are hallmarks of a high-performance sensing platform. Such results correspond to the earlier research, which has determined such band gap thresholds to be the most effective with 2D nanomaterials utilized in chemical sensing.

The difference in $E_F$ of the doped Gr systems between -4.904 eV and -5.549 eV indicates significant changes in the electronic properties of the various dopant atoms. The changes in the values of $E_F$ are also signs of charge redistribution at the Gr surface, due to differences in the electronegativity and the orbital hybridization between C and the incorporated dopants (Ni, Si, S, and Co) [54]. Reduced Fermi levels imply an improved electron-withdrawing behavior of the dopants, causing a downward change in the electronic states towards greater binding energies.

The significance of this behavior in gas sensing applications [55], is that variations in $E_F$ have a direct influence on the charge transfer dynamics between the adsorbed HCN molecule and the substrate and, therefore, sensor response, conductivity modulation, and sensitivity. The tunability of the electronic landscape of the Gr indicated by the range of $E_F$ is essential to maximize selectivity and responsiveness in HCN detection. Figure 2 shows that the DOS spectra suggest a broad impact on the electronic structure of Gr in the context of the atomic doping.

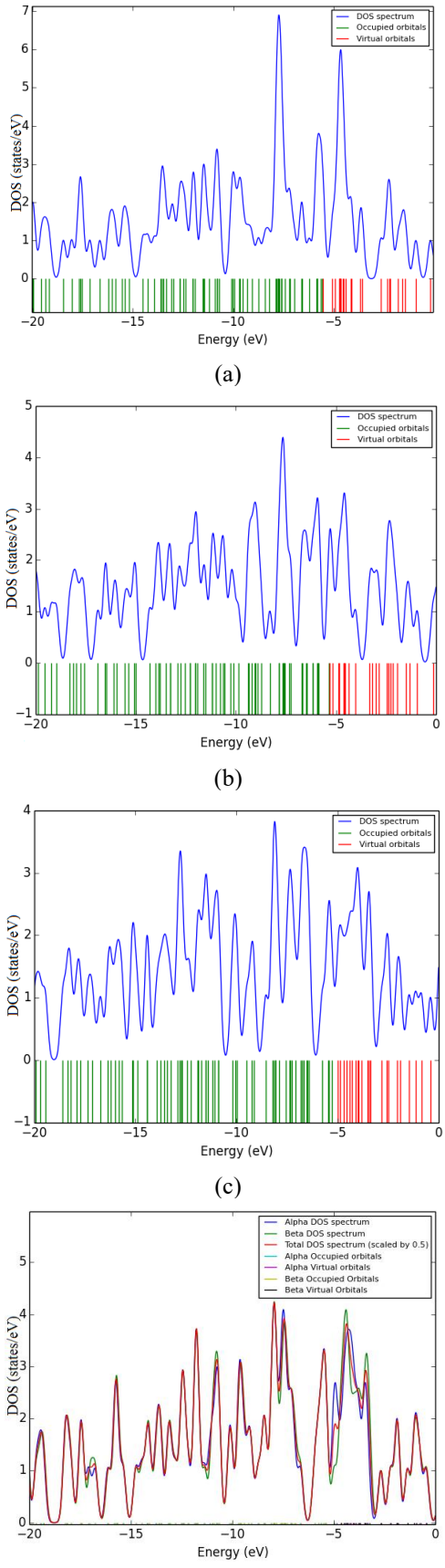


**Figure 2.** Density of states (DOS) plots for Gr systems doped with different atoms: (a) Ni-Gr, (b) Si-Gr, (c) S-Gr, and (d) Co-Gr

When transition and non-transition metal dopants (Ni, Si, S, and Co) are introduced, the density and distribution of electronic states around the Fermi level are changed significantly. In Ni-doped Gr (Ni-Gr) (Figure 2(a)), the DOS shows sharp and high intensity peaks in the valence region near the Fermi level, indicating high hybridization of Ni 3d orbitals with the π state of graphene.

The outcome of this hybridization is the increase in DOS and partial filling of the states at the Fermi level that may lead to an increase in electrical conductivity and surface reactivity.

In the case of Si-doped Gr (Si–Gr) (Figure 2(b)), the DOS spectrum shows a smoother distribution of states, with moderate peak features that spread across the valence band. The incorporation of Si-being from group IV-results in minimum disruption to the π-conjugated system, retains a semi-metallic character, and adds a slight asymmetry to orbital distributions. The observed DOS features in Figure 2(c) for S-doped Gr (S-Gr) show strong peaks mainly in the valence band region, which suggests a high orbital density and delocalization of electrons is observed over the wide energy range.

The sharp peaks near the Fermi level indicate that the dopant orbitals are strongly hybridized with the π-system of Gr. Figure 2(d) for Co-doped Gr (Co-Gr) indicates that virtual orbital features of the conduction band region indicate the presence of unoccupied electronic states that can potentially participate in charge transfer during adsorption processes, especially in gas sensing or catalytic processes. Overall, the DOS analysis has verified that Co-doping changes the electronic properties of Gr to introduce localized states and mild spin polarization, potentially increasing its chemical reactivity and adsorption properties in the environmental or sensing context [56].

Table 2 shows the calculated adsorption energies, $E_g$, HOMO LUMO energies, and Fermi energies of all the systems studied. We find that the addition of Ni, Si, S, and Co dopants into the Gr lattice causes significant changes in the structural and electronic properties of the lattice and hence in its interaction with HCN molecules. It is worth noticing that the recorded changes in the electron band structures and frontier orbital energies emphasize the tunability of doped Gr, which makes it suitable to selectively adsorb gases with higher efficiency [57]. Optimized adsorption modes of HCN on Gr surfaces doped with Ni, Si, S, and Co are depicted in Figure 3(a) to (d), respectively.

The geometries of the adsorption are contrasted to show clear differences in the bonding distances and angular orientation with respect to the Gr plane. In particular, the adsorption distance between the C atom of HCN and dopant atoms (C-Ni, C-Si, C-S, and C-Co) has been calculated as 1.97 Å, 1.97 Å, 1.83 Å [58], and 1.99 Å, respectively. These values imply that there is a bit stronger interaction in the case of S doping with the shortest bond length.

Moreover, the angles of corresponding adsorption that are established between the Gr plane and the C-dopant bonds are 106°, 87°, 97°, and 91°, respectively. The extreme angle difference between the Ni-doped system (106°) could suggest that there is an out-of-plane distortion, which may affect the electronic characteristics of the adsorption site. All of these structural parameters underscore the dopant-dependent nature of HCN adsorption, which might be of great importance in designing Gr-based sensors or catalytic platforms.

The calculated adsorption energies of HCN on Gr surfaces doped with Ni, Si, S, and Co are -0.956 eV [44], -0.832 eV, -0.229 eV, and -0.559 eV, respectively. These values indicate the different levels of interaction of strength between the HCN molecule and the doped Gr substrates. Interestingly, adsorption energies of the Ni- and Si-doped systems suggest a chemisorption mechanism, which also predicts strong binding indicative of chemical adsorption, reflecting the sensitivity of adsorption properties to computational techniques and structural models.

However, the values of the $E_{ad}$ of the present work justify the conclusion that HCN binds to the doped Gr surfaces significantly [59]. This great interaction highlights the possibility of Ni-Gr, Si-Gr, S-Gr, and Co-Gr as good platforms to detect HCN, which could provide promising leads to the development of high-performance gas sensors. Although these differences exist, the large values of $E_{ad}$ that were realized in this research attest to the fact that HCN reacts well with the doped Gr substrates, especially when Ni and Si dopants are present.

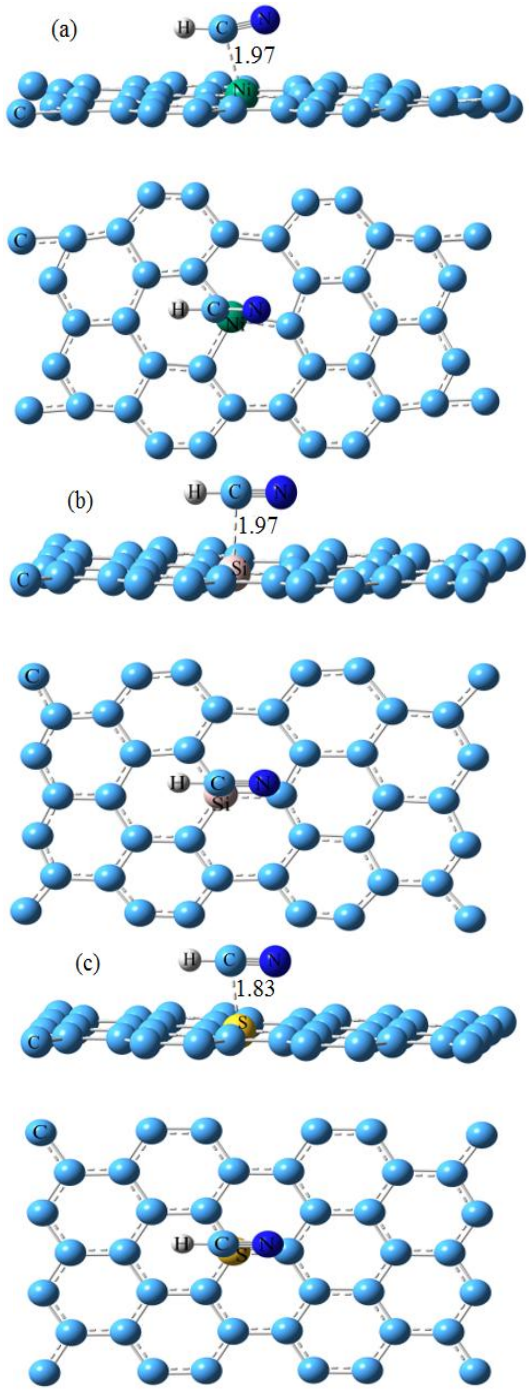

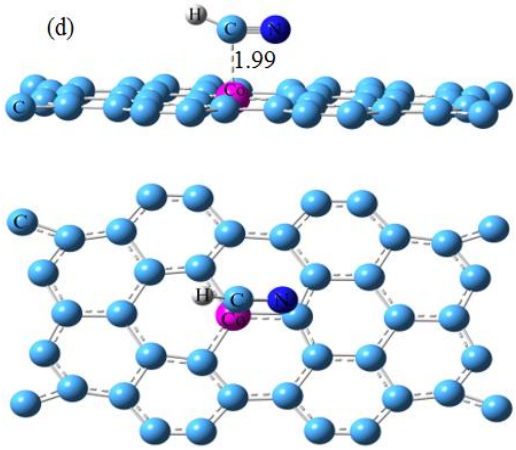


**Figure 3.** Optimized geometries (top and side views) and key bond lengths of hydrogen cyanide (HCN) gas adsorbed on Gr doped with (a) Ni, (b) Si, (c) S, and (d) Co atoms

This high binding increases the selectivity and sensitivity of the material to HCN molecules, and these doped Gr systems are good candidates to be used in gas sensing. The ability to design the properties of adsorption by controlling doping is a strategic direction for the optimization of Gr-based sensors in the detection of toxic gases. The results can be added to the increasing number of studies aimed at the functionalization of Gr towards environmental monitoring and industrial safety.

Table 2 results indicate that the $E_g$ of the Ni-Gr system post gas adsorption of HCN is essentially the same (0.034 eV) as the pre-adsorption of the system, and that the electronic perturbation is insignificant. Typically, the HCN molecule and the saturated Ni site develop a strong chemical bond. As this reaction does not break the long-range π bonds that occur across the Gr basal plane, the electronic states close to the Fermi level that govern the bandgap are not largely affected. This is the reason why this system possesses much structural stability and does not exhibit any considerable electronic transitions.

**Table 2.** Electronic and structural characteristics of hydrogen cyanide (HCN) molecule adsorption on Gr doped with Ni, Si, S, and Co atoms

| Materials | $E_{ad}$ (eV) | $E_g$ (eV) | $E_{HOMO}$ (eV) | $E_{LUMO}$ (eV) | $E_F$ (eV) |
|---|---|---|---|---|---|
| Ni-Gr | -0.956 | 0.034 | -5.559 | -5.525 | -5.542 |
| Si-Gr | -0.832 | 0.048 | -5.332 | -5.284 | -5.308 |
| S-Gr | -0.229 | 0.011 | -5.300 | -5.289 | -5.294 |
| Co-Gr | -0.559 | 0.159 | -5.677 | -5.518 | -5.597 |

Note: Adsorption energy ($E_{ad}$); Energy gap ($E_g$); Highest occupied molecular orbital (HOMO); Lowest unoccupied molecular orbital (LUMO); Fermi energy ($E_F$).

As a result, the π–π conjugation and the DOS near the Fermi level are not significantly disturbed. After adsorption of HCN gas on S-Gr, a significant decrease in the electronic $E_g$ was noted, as indicated in Table 2. The value of $E_g$ following adsorption was determined to be less than that of S-Gr, this means that an interaction between the HCN molecule and doped Gr surface triggers the narrowing of the band gap [60]. Such drop in $E_g$ can be attributed to charge transfer processes and orbital hybridization between the S-Gr substrate and the adsorbed HCN molecule. Specifically, a localized state near the Fermi level corresponds to the S atoms interacting with the HCN molecular orbitals when adsorbed.

The perturbation of such interaction on the electronic structure of the Gr surface is a smaller $E_g$ between the conduction and valence bands. This band gap modulation enhances the electronic sensitivity of the material, which validates S-Gr as a good choice to use in HCN sensing applications. Conversely, the electronic $E_g$ of HCN gas adsorbed on Co–Gr and Si–Gr increased compared to the pristine forms. This upward shift of $E_g$ indicates that the interaction of the HCN molecules with the doped Gr surfaces causes an alteration of the electronic structure, which increases the $E_g$ between the valence and conduction bands.

The resulting enhancement may be explained by the characteristics of the dopant atoms, Si and Co that affect the redistribution of charge and orbital alignment during adsorption. Specifically, HCN adsorption can cause a passivation effect or decreased DOS near the Fermi level, thereby preventing electronic transitions and raising the band gap. An examination of how the HCN molecules' adsorption influences the electronic characteristics of doped Gr systems shows that a wide variety of interactions exists, which largely depend on the active site of the dopant. The findings indicate that $E_{ad}$ and the bandgap shift are finely tuned and that the Ni-Gr system has the greatest binding energy (-0.956 eV), owing to the strong atomic orbital interaction, and that the bandgap changes are small, implying that the interactions are highly stabilizing without bringing a radical change in the electronic structure of the system.

Conversely, the S-Gr system has a strong variation in $E_g$ (0.311 to 0.011 eV), and this is due to the critical role of charge transfer between the molecule and the doped surface, as this is the main cause of the change in the electrical properties of the system despite a reduction in $E_{ad}$. Using these data, Co-Gr system is the most appropriate and optimal solution; it balances appropriate adsorption stability (-0.559 eV) and an effective ability for modulating $E_g$ (between 0.129 and 0.159 eV), which allows it to provide an exemplary electronic response and at the same time ensure the stability of the chemical bond.

The calculated $E_F$ values demonstrate that there were different adsorption-induced electronic responses with different dopants. In the case of Ni-Gr and Si-Gr systems, $E_F$ post-HCN adsorption is greater than the pre-adsorption value. This increase reflects an electron donation reaction of the HCN molecules to the substrate, which is effectively the raise in the free carrier concentration and the Fermi level [61]. This indicates weak-to-moderate charge transfer interactions, which may take place in physisorption regimes and chemisorption regimes. Conversely, in the case of the S-Gr and Co-Gr systems, $E_F$ decreases after adsorbing HCN. This downward shift indicates a reverse direction charge transfer-electrons are transferred by the substrate to the HCN molecule [62].

In this case, HCN is the electron acceptor, which decreases the electron density in the substrate and decreases $E_F$. This dual behavior is supported by the electronic structure of HCN. The $E_{HOMO}$ value of -5.677 eV would mean its capability for electron donation, whereas the $E_{LUMO}$ of -5.284 eV would mean it can accept electrons. As a result, the direction and magnitude of charge transfer are dictated by the relative orientations of the molecular frontier orbitals with the Fermi level of the doped Gr, which is again sensitive to the nature of the dopant atom. This is the reason why the same gas molecule has a donor behavior towards S–Gr and Co–Gr and acceptor

behavior towards Ni–Gr and Si–Gr and eventually modifies the $E_F$ in opposite directions.

Figure 4 shows the DOS spectra of the materials under study, as a function of energy between the values of –20 eV and 0 eV. The horizontal axis is the energy levels (in electron volts), and the vertical scale shows the DOS, given in the number of states per eV. The blue curve is the total DOS, the vertical lines are the occupied molecular orbitals (green), and the virtual (unoccupied) orbitals (red). The occupied orbitals represent the distribution of electrons in the ground state, and the virtual orbitals represent the energy levels that are available for electronic excitation. This difference is crucial in the study of the electronic behavior of the material, especially as concerns its chemical reactivity and optical characteristics [63].

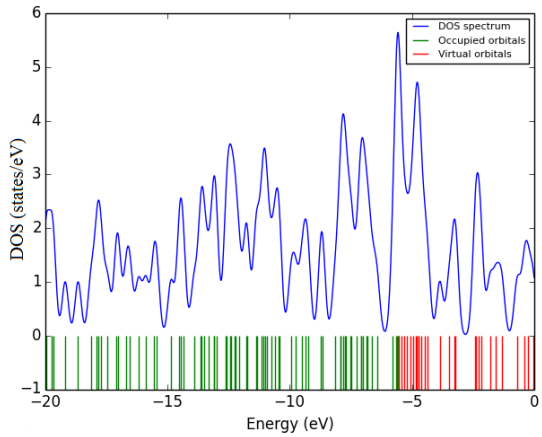


(a)

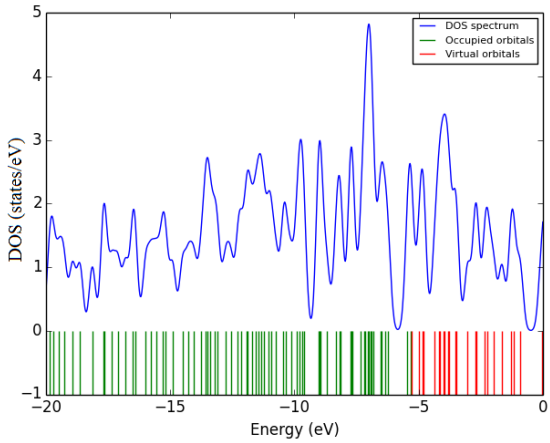


(b)

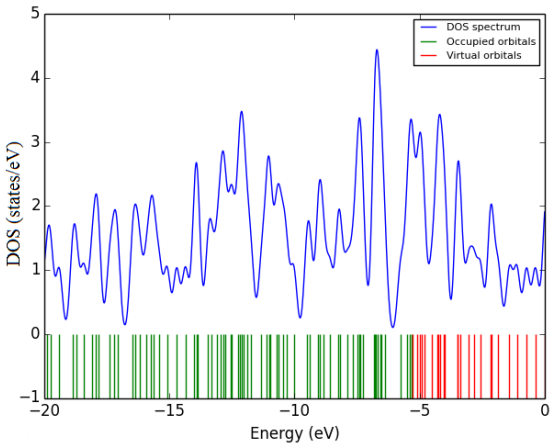


(c)

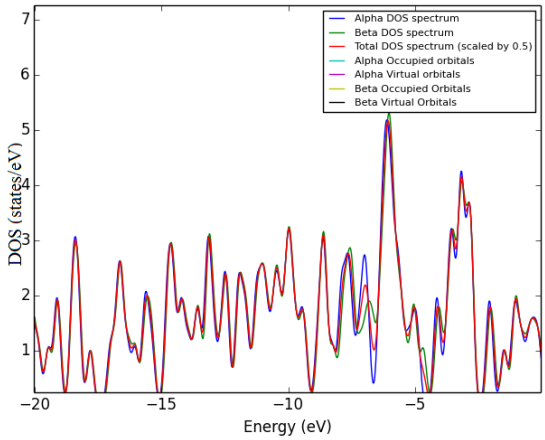


(d)

**Figure 4.** Density of states (DOS) spectra for hydrogen cyanide (HCN) gas adsorbed on Gr doped with (a) Ni, (b) Si, (c) S, and (d) Co atoms, demonstrating the influence of dopant type on the electronic response of the system

The DOS profile gives an insight into the electronic structure, such as the existence or lack of a band gap directly related to the conductivity of the material and its possible use in electronic or optoelectronic devices [64]. In the case of the Ni–Gr/HCN system (Figure 4(a)), a redistribution of the DOS near the Fermi level is evident, as compared to that of doped Gr, as a result of HCN adsorption on the electronic structure. Both the downward and upward shifts in the DOS intensity near the $E_F$ indicate charge transfer interactions between the adsorbate and substrate, which are in line with the observed reduction in the $E_F$, which is an indication of electron transfer between the substrate and the adsorbate. The same redistribution of states is found in the Si–Gr/HCN system (Figure 4(b)), although the DOS peaks around the $E_F$ are not as strong as in the Ni–Gr/HCN system.

This implies that there are relatively weaker hybridizations between the Si–Gr substrate and HCN molecular orbitals, but $E_F$ shift still indicates that there is a net electron transfer to the HCN molecule. The LUMO and HOMO in relation to the $E_F$ suggest a possibility of both donation and acceptance of electrons, which corresponds to the dual donor–acceptor nature of HCN based on its $E_{HOMO}$ and $E_{LUMO}$ values. The DOS spectrum of the S–Gr/HCN system is illustrated in Figure 4(c). The somewhat broad distribution of occupied states implies a robust hybridization of the electronic states of the S–Gr substrate and those of the adsorbed HCN molecule.

Nevertheless, the DOS intensity near the Fermi level is moderate with respect to Ni–Gr/HCN, which means that there is a weaker charge transfer and orbital coupling strength. Such an observation is consistent with the smaller predicted shift in the Fermi level of S–Gr with HCN adsorption, which suggests that the interaction is not as electronically perturbative as is the case of the Ni-doped. Figure 4(d) shows DOS spectrum of the Co–Gr/HCN system. The occupied and virtual orbital distributions show that adsorption causes minor changes around the Fermi level that may affect electrical conductivity and sensing of Co–Gr/HCN surface.

The FMO analysis of the HCN adsorption on metal-doped Gr (Ni, Si, S, and Co) shows a stable trend of electronic interaction, though with some differences being determined by the nature of the dopants. The HOMO distribution on all substrates (Figure 5) is highly localized around both the N

atom of the HCN molecule and the Gr framework as well, and this demonstrates a universal charge donation process by the substrate to the adsorbate. On the other hand, the LUMO distribution, which is highly delocalized on both the substrate and the gas molecule, always points to the contribution of the HCN $\pi^*$ antibonding orbitals to the adsorption process.

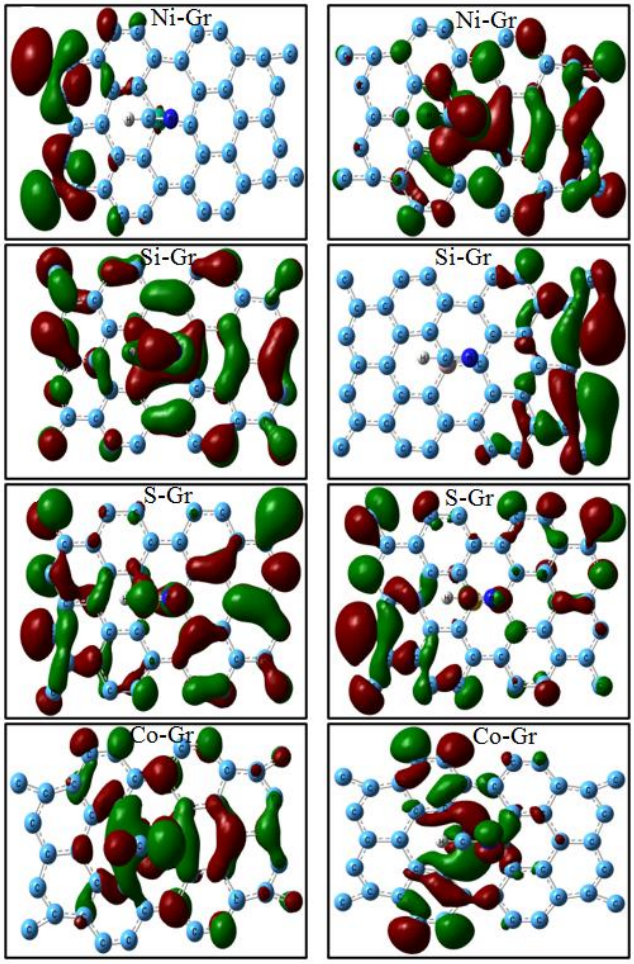


**Figure 5.** FMO distributions (HOMO on the left, LUMO on the right) of HCN gas adsorbed on Gr doped with Ni, Si, S, and Co atoms

Note: Frontier molecular orbital (FMO); Highest occupied molecular orbital (HOMO); Lowest unoccupied molecular orbital (LUMO); hydrogen cyanide (HCN).

These features are common, but the spatial distribution of electron density differs greatly depending on the dopant: in the cases of Ni, Si, and S-doped systems, the LUMO density is concentrated around the C atom of HCN, which is likely to provide a direct interaction pathway.

In Co–Gr, however, the LUMO distribution is more high near the atoms of Gr C, which shows a different electronic environment, and makes two-way charge transfer. The existence of such spatial overlaps and orbital complementarities emphasizes the high electronic coupling of such systems that should be taken into account in enhancing selectivity and sensitivity of such materials in the detection of HCN.

## 4. CONCLUSIONS

This study indicates that doping Gr with select transition metal or heteroatom is a very promising approach in the modulation of its electronic properties and increasing its adsorption capacity of hazardous HCN gas. We have found that the Si–Gr and Ni–Gr systems have much stronger chemical interactions with HCN than their S–Gr and Co–Gr systems, and are better candidates to develop high-sensitivity gas sensors.

These improved interactions are confirmed using advanced electronic structure analyses, such as DOS and FMO, to show that these enhanced interactions result in a large charge redistribution near the Fermi level, which is essential to sensing applications, but in such configurations as Ni–Gr, the chemical bonding is performed without disrupting the extended $\pi$-conjugation of the Gr basal plane, and therefore maintaining a high structural stability even in the presence of an adsorption process. Taken together, these observations explain the principles of how molecules and surfaces interact at the atomic scale, and provide a foundation on which the rational design of next-generation, tuned nanomaterials can be used to monitor the environment and achieve workplace safety.

## REFERENCES


[1] Jang, J.S., Winter, L.R., Kim, C., Fortner, J.D., Elimelech, M. (2021). Selective and sensitive environmental gas sensors enabled by membrane overlayers. Trends in Chemistry, 3(7): 547-560. https://doi.org/10.1016/j.trechm.2021.04.005

[2] Kamarchuk, G., Pospelov, A., Kamarchuk, L., Belan, V., Herus, A., Savytskyi, A., Faulques, E. (2023). Quantum mechanisms for selective detection in complex gas mixtures using conductive sensors. Scientific Reports, 13(1): 21432. https://doi.org/10.1038/s41598-023-48207-0

[3] Chen, H., Li, H.Y., Ren, H., Wang, H., Chen, P., Guo, D., Liu, H. (2025). Highly sensitive and full range laser methane gas detector based on automatic wavelength-switching algorithm. Sensors and Actuators B: Chemical, 437: 137699. https://doi.org/10.1016/j.snb.2025.137699

[4] Devi, P. (2021). Hydrogen cyanide: Risk assessment, environmental, and health hazard. In Hazardous Gases, Academic Press, pp. 183-195. https://doi.org/10.1016/B978-0-323-89857-7.00010-4

[5] Rashid, H.A., Hassan, N.E. (2024). Review of toxic gases and their impact on human health. Journal of Applied Bio-Sciences, 1(4): 7-12. https://doi.org/10.55559/jjbrpac.v1i4.398

[6] Lachowicz, J.I., Alexander, J., Aaseth, J.O. (2024). Cyanide and cyanogenic compounds—Toxicity, molecular targets, and therapeutic agents. Biomolecules, 14(11): 1420. https://doi.org/10.3390/biom14111420

[7] Cheng, S., Chen, J., Zeng, W., Zhou, Q. (2023). The adsorption and sensing mechanism of toxic gases HCN, NO2, NH3 and Cl2 on Mo, Ag-modified WSe2 monolayer: insights from the first-principles computations. Materials Today Communications, 35: 105906. https://doi.org/10.1016/j.mtcomm.2023.105906

[8] Kanaabi, M., Namakula, F.B., Nuwamanya, E., Kayondo, I.S., Muhumuza, N., Wembabazi, E., Kawuki, R.S. (2024). Rapid analysis of hydrogen cyanide in fresh cassava roots using NIRS and machine learning algorithms: Meeting end user demand for low

cyanogenic cassava. The Plant Genome, 17(2): e20403. https://doi.org/10.1002/tpg2.20403
[9] Cai, S., Zhou, Q., Zhao, Z., Liu, X., Ju, W., Hou, J. (2024). Density functional theory analysis of the sensitivity of silicene/graphene heterostructures toward HCN. Colloids and Surfaces A: Physicochemical and Engineering Aspects, 681: 132799. https://doi.org/10.1016/j.colsurfa.2023.132799
[10] Bläsing, K., Harloff, J., Schulz, A., Stoffers, A., Stoer, P., Villinger, A. (2020). Salts of HCN-cyanide aggregates: $[CN(HCN)2]^-$ and $[CN(HCN)3]^-$. Angewandte Chemie International Edition, 59(26): 10508-10513. https://doi.org/10.1002/anie.201915206
[11] To, D.T.H., Myung, N.V. (2024). Critical review of hydrogen cyanide (HCN) sensors and their applications. Sensors and Actuators Reports, 8: 100254. https://doi.org/10.1016/j.snr.2024.100254
[12] Tohidi, T., Sattarian, H., Tohidi, S. (2022). A DFT study of gas molecules adsorption on intrinsic and Cu-doped graphene gas nanosensors. Physica Scripta, 97(10): 105807. https://doi.org/10.1088/1402-4896/ac8eee
[13] Li, K., Li, N., Yan, N., Wang, T., Zhang, Y., Song, Q., Li, H. (2020). Adsorption of small hydroCs on pristine, N-doped and vacancy graphene by DFT study. Applied Surface Science, 515: 146028. https://doi.org/10.1016/j.apsusc.2020.146028
[14] Liu, D., Wei, S., Wang, D. (2022). Sensitivity comparison between monolayer graphene and multilayer graphene. Journal of New Materials for Electrochemical Systems, 25(3): 1-7. https://doi.org/10.14447/jnmes.v25i3.a10
[15] Zhang, Q., Xu, Y., Zhang, J.A., Lu, Y., Tian, J. (2021). Graphene functionalized by doping and defects for gas sensor application. Sensors & Materials, 33: 1245-1258. https://doi.org/10.18494/SAM.2021.3296
[16] Wu, Y., Chen, X., Weng, K., Arramel, et al. (2021). Highly sensitive and selective gas sensor using heteroatom doping graphdiyne: A DFT study. Advanced Electronic Materials, 7(7): 2001244. https://doi.org/10.1002/aelm.202001244
[17] Zhu, Y., Wu, J., Han, L., Wang, X., Li, W., Guo, H., Wei, H. (2020). Nanozyme sensor arrays based on heteroatom-doped graphene for detecting pesticides. Analytical Chemistry, 92(11): 7444-7452. https://doi.org/10.1021/acs.analchem.9b05110
[18] Korivand, M., Zamani, M. (2021). Surface modification of graphene by coupling with electron deficient radicals. Journal of Solid-State Chemistry, 294: 121851. https://doi.org/10.1016/j.jssc.2020.121851
[19] Guo, J., Liu, H., Li, D., Wang, J., Djitcheu, X., He, D., Zhang, Q. (2022). A minireview on the synthesis of single atom catalysts. RSC Advances, 12(15): 9373-9394. https://doi.org/10.1039/D2RA00657J
[20] Chen, Z., Zhang, P. (2022). Electronic structure of single-atom alloys and its impact on the catalytic activities. ACS Omega, 7(2): 1585-1594. https://doi.org/10.1021/acsomega.1c06067
[21] Deji, R., Verma, A., Kaur, N., Choudhary, B.C., Sharma, R.K. (2022). Adsorption chemistry of co-doped graphene nanoribbon and its derivatives towards C based gases for gas sensing applications: Quantum DFT investigation. Materials Science in Semiconductor Processing, 146: 106670. https://doi.org/10.1016/j.mssp.2022.106670
[22] Armillotta, F., Naderasli, P., Chesnyak, V., Brune, H. (2024). Reverse spillover dominating CO adsorption on single cobalt atoms in graphene divacancies. The Journal of Physical Chemistry C, 129(10): 4915-4922. https://doi.org/10.1021/acs.jpcc.4c07088
[23] Javan, M., Jorjani, R., Soltani, A.R. (2020). Theoretical study of nitrogen, boron, and co-doped (B, N) armchair graphene nanoribbons. Journal of Molecular Modeling, 26(4): 64. https://doi.org/10.1007/s00894-020-4307-x
[24] Deji, R., Jyoti, R., BC, C., Ramesh, K.S. (2021). Enhanced sensitivity of graphene nanoribbon gas sensor for detection of oxides of nitrogen using boron and phosphorus co-doped system: A first principles study. Sensors and Actuators A: Physical, 331: 112897. https://doi.org/10.1016/j.sna.2021.112897
[25] Zhou, Z., Song, J., Xie, Y., Ma, Y., et al. (2025). DFT calculation for organic semiconductor-based gas sensors: Sensing mechanism, dynamic response and sensing materials. Chinese Chemical Letters, 36(6): 110906. https://doi.org/10.1016/j.cclet.2025.110906
[26] Zhao, Z., Jiang, Y., Lin, W., Nan, W., et al. (2025). From discovery to optimization: Data-driven development of NH3 sensing materials validated by experiments and DFT. Journal of Hazardous Materials, 495: 139169. https://doi.org/10.1016/j.jhazmat.2025.139169
[27] Devi, K., Ganesan, A., Singh, K.K. (2025). Enhancing the vibrational sensitivity of graphene via substitutional doping for multimodal gas sensing applications–A DFT study. Physica Scripta, 100(10): 105906. https://doi.org/10.1088/1402-4896/ae0987
[28] Saunders, B., Hörmann, L., Maurer, R.J. (2025). Comprehensive structure exploration and thermodynamics of heteroatom doped graphene superstructures. arXiv preprint, arXiv:2509.08352. https://doi.org/10.48550/arXiv.2509.08352
[29] Ullah, S., Shi, Q., Zhou, J., Yang, X., Ta, H.Q., Hasan, M., Rümmeli, M.H. (2020). Advances and trends in chemically doped graphene. Advanced Materials Interfaces, 7(24): 2000999. https://doi.org/10.1002/admi.202000999
[30] Chenwittayakhachon, A., Jitapunkul, K., Nakpalad, B., Worrayotkovit, P., Namuangruk, S., Sirisinudomkit, P., Iamprasertkun, P. (2023). Machine learning approach to understanding the 'synergistic' pseudocapacitive effects of heteroatom doped graphene. 2D Materials, 10(2): 025003. https://doi.org/10.1088/2053-1583/acaf8d
[31] Banglani, T.H., Chandio, I., Khilji, M.U.N., Ibrar, A., et al. (2024). Graphene-based nanocomposites for gas sensors: Challenges and opportunities. Reviews in Inorganic Chemistry, 44(3): 385-408. https://doi.org/10.1515/revic-2023-0033
[32] Choi, J.H., Lee, J., Byeon, M., Hong, T.E., Park, H., Lee, C.Y. (2020). Graphene-based gas sensors with high sensitivity and minimal sensor-to-sensor variation. ACS Applied Nano Materials, 3(3): 2257-2265. https://doi.org/10.1021/acsanm.9b02378
[33] Deji, R., Jyoti, R., BC, C., Ramesh, K.S. (2022). A theoretical study of HCN adsorption and width effect on co-doped armchair graphene nanoribbon. Computational and Theoretical Chemistry, 1209: 113592. https://doi.org/10.1016/j.comptc.2022.113592
[34] Siddique, S.A., Sajid, H., Gilani, M.A., Ahmed, E., Arshad, M., Mahmood, T. (2022). Sensing of SO3, SO2, H2S, NO2 and N2O toxic gases through aza-macrocycle via DFT calculations. Computational and Theoretical

Chemistry, 1209: 113606. https://doi.org/10.1016/j.comptc.2022.113606
[35] Khudair, S.A.M. (2025). Harmful gas molecule detection using lithium doped graphene: Theoretical analysis of adsorption and gas-sensing properties. Annales de Chimie - Science des Matériaux, 49(6): 703-712. https://doi.org/10.18280/acsm.490612
[36] Taha, H.O., El Mahdy, A.M., Lebda, H.I., El-Wanees, E.A. (2026). Electronic and adsorption properties of the zigzag-edged triangle graphene flakes doped with transition metal: DFT investigation. Optical and Quantum Electronics, 58(2): 89. https://doi.org/10.1007/s11082-025-08628-9
[37] Shrestha, M.K., Dawadi, N., Shrestha, M.R., Sedai, P., Adhikari, S., Lamichhane, H.P. (2025). Conformational study on various tripeptides containing threonine: A density functional theory approach. Amrit Research Journal, 6(1): 1-14. https://doi.org/10.3126/arj.v6i1.87495
[38] Khadka, M., Sah, M., Chaudhary, R., Sahani, S.K., Sahani, K., Pandey, B.K., Pandey, D. (2025). Spectroscopic, quantum chemical, and topological calculations of the phenylephrine molecule using density functional theory. Scientific Reports, 15(1): 208. https://doi.org/10.1038/s41598-024-81633-2
[39] Devi, P.K., Singh, K.K. (2023). Enhancement of electronic and optical characteristics of graphene by doping with transition metals–DFT method. Physica B: Condensed Matter, 669: 415309. https://doi.org/10.1016/j.physb.2023.415309
[40] Khudair, S., Jappor, H. (2020). Adsorption of gas molecules on graphene doped with mono and dual boron as highly sensitive sensors and catalysts. Journal of Nanostructures, 10(2): 217-229. https://doi.org/10.22052/JNS.2020.02.003
[41] Gui, Y., Peng, X., Liu, K., Ding, Z. (2020). Adsorption of C2H2, CH4 and CO on Mn-doped graphene: Atomic, electronic, and gas-sensing properties. Physica E: Low-dimensional Systems and Nanostructures, 119: 113959. https://doi.org/10.1016/j.physe.2020.113959
[42] Zhang, M.Z., Yang, J., Dai, K.Y., Wen, J. (2026). Photoactive H-bonding EDA complex in radical chemistry. Chemistry–A European Journal, 32(13): e70708. https://doi.org/10.1002/chem.70708
[43] Talha, A., Shihab, F.H., Ahmed, M.T., Al Roman, A., Kowser, Z., Roy, D. (2024). Density functional theory study of the adsorption and dissociation of OF2 and O3 gases on the surface of pristine and Al, Ti and Cr doped graphene. AIP Advances, 14(7): 075112. https://doi.org/10.1063/5.0214735
[44] Zhu, P., Zhu, Y., Yu, W., Zhao, J. (2025). Adsorption properties of HCN, NO, and NH3 on transition metal-doped AA-stacked bilayer graphene: First principle study. Molecular Physics, 123(4): e2384438. https://doi.org/10.1080/00268976.2024.2384438
[45] Scotland, P., Eddy, L., Chen, J., Chen, W., et al. (2025). Heteroatom-Substituted Reflashed Graphene. ACS Nano, 19(12): 11987-11998. https://doi.org/10.1021/acsnano.4c16959
[46] Gao, X., Zhou, Q., Wang, J., Xu, L., Zeng, W. (2020). Performance of intrinsic and modified graphene for the adsorption of H2S and CH4: A DFT study. Nanomaterials, 10(2): 299. https://doi.org/10.3390/nano10020299
[47] Zhou, Y., He, X., Li, M. (2025). Roles of doping in enhancing the performance of graphene/graphene-like semiconductors. AIP Advances, 15(1): 015214. https://doi.org/10.1063/5.0248505
[48] Deokar, G., Jin, J., Schwingenschlögl, U., Costa, P.M. (2022). Chemical vapor deposition-grown nitrogen-doped graphene's synthesis, characterization and applications. npj 2D Materials and Applications, 6(1): 14. https://doi.org/10.1038/s41699-022-00287-8
[49] Solanki, K., Majumder, M.K. (2022). Hydrogen cyanide gas sensor using doped/undoped graphene nanoribbon. In 2022 5th International Conference on Multimedia, Signal Processing and Communication Technologies (IMPACT), pp. 1-5. https://doi.org/10.1109/IMPACT55510.2022.10029158
[50] Joseph, S., Thomas, S., Mohan, J., Kumar, A.S., Jayasree, S.T., Thomas, S., Kalarikkal, N. (2021). Theoretical study on tuning band gap and electronic properties of atomically thin nanostructured MoS2/metal cluster heterostructures. ACS Omega, 6(10): 6623-6628. https://doi.org/10.1021/acsomega.0c05274
[51] Wang, H., Yam, K.M., Jiang, Z., Guo, N., Zhang, C. (2024). Structure phase change induced by nonequilibrium effects in molecular-scale junctions. Physical Review B, 110(12): L121405. https://doi.org/10.1103/PhysRevB.110.L121405
[52] Feng, S., Lin, Z., Gan, X., Lv, R., Terrones, M. (2017). Doping two-dimensional materials: Ultra-sensitive sensors, band gap tuning and ferromagnetic monolayers. Nanoscale Horizons, 2(2): 72-80. https://doi.org/10.1039/C6NH00192K
[53] Park, J., Xia, Y., Ozoliņš, V., Jain, A. (2021). Optimal band structure for thermoelectrics with realistic scattering and bands. npj Computational Materials, 7(1): 43. https://doi.org/10.1038/s41524-021-00512-w
[54] Shih, P.H., Do, T.N., Gumbs, G., Lin, M.F. (2020). Electronic and optical properties of doped graphene. Physica E: Low-Dimensional Systems and Nanostructures, 118: 113894. https://doi.org/10.1016/j.physe.2019.113894
[55] Tian, H., Wang, L., Sofer, Z., Pumera, M., Bonanni, A. (2016). Doped graphene for DNA analysis: The electrochemical signal is strongly influenced by the kind of dopant and the nucleobase structure. Scientific Reports, 6(1): 33046. https://doi.org/10.1038/srep33046
[56] Paidi, V.K., Jung, E., Lee, J., Lee, A.T., et al. (2023). Robust room temperature ferromagnetism in cobalt doped graphene by precision control of metal ion hybridization. Advanced Functional Materials, 33(3): 2210722. https://doi.org/10.1002/adfm.202210722
[57] Mirzaei, A., Bharath, S.P., Kim, J.Y., Pawar, K.K., Kim, H.W., Kim, S.S. (2023). N-Doped Graphene and its derivatives as resistive gas sensors: An overview. Chemosensors, 11(6): 334. https://doi.org/10.3390/chemosensors11060334
[58] Zhou, Q., Ju, W., Su, X., Yong, Y., Li, X., Fu, Z., Wang, C. (2017). Adsorption sensitivity of graphane decorated with B, N, S, and Al towards HCN: A first-principles study. RSC Advances, 7(69): 43521-43530. https://doi.org/10.1039/C7RA08579F
[59] Bekhit, M.M., Mudhafar, M., Abass, Z.A., Kanjariya, P., et al. (2025). Aluminum-doped T-graphene: An innovative platform for enhanced sensitivity in hydrogen cyanide detection. Chemical Physics, 593: 112648.

https://doi.org/10.1016/j.chemphys.2025.112648
[60] Chen, L., Li, X., Ma, C., Wang, M., Zhou, J. (2017). Interaction and quantum capacitance of nitrogen/sulfur co-doped graphene: A theoretical calculation. The Journal of Physical Chemistry C, 121(34): 18344-18350. https://doi.org/10.1021/acs.jpcc.7b04551
[61] Sahithi, A., Sumithra, K. (2025). Electronic and adsorption characteristics of hydrogen cyanide (HCN) and isocyanide (HNC) on intrinsic and doped phosphorene. AIP Advances, 15(2): 025230. https://doi.org/10.1063/5.0220697
[62] Shi, L.B., Wang, Y.P., Dong, H.K. (2015). First-principle study of structural, electronic, vibrational and magnetic properties of HCN adsorbed graphene doped with Cr, Mn and Fe. Applied Surface Science, 329: 330-336. http://doi.org/10.1016/j.apsusc.2014.12.172
[63] Shen, H., Head-Gordon, M. (2024). Occupied-virtual orbitals for chemical valence with applications to charge transfer in energy decomposition analysis. The Journal of Physical Chemistry A, 128(26): 5202-5211. https://doi.org/10.1021/acs.jpca.4c02364
[64] Woods-Robinson, R., Han, Y., Zhang, H., Ablekim, T., Khan, I., Persson, K.A., Zakutayev, A. (2020). Wide band gap chalcogenide semiconductors. Chemical Reviews, 120(9): 4007-4055. https://doi.org/10.1021/acs.chemrev.9b00600

## NOMENCLATURE

| | |
|---|---|
| Co-Gr | Co-doped graphene |
| DFT | density functional theory |
| DOS | density of states |
| $E_{ad}$ | adsorption energy, eV |
| $E_F$ | Fermi energy, eV |
| $E_g$ | energy gap, eV |
| FMO | frontier molecular orbital |
| GGA | generalized gradient approximation |
| Gr | graphene |
| HOMO | highest occupied molecular orbital |
| LUMO | lowest unoccupied molecular orbital |
| Ni-Gr | Ni-doped graphene |
| PBE | Perdew-Burke-Ernzerhof |
| S-Gr | S-doped graphene |
| Si-Gr | Si-doped graphene |